GEOPHYSICAL RESEARCH LETTERS, VOL. 34, L12812, doi:10.1029/2007GL030111, 2007

First observations of iodine oxide from space

Alfonso Saiz-Lopez,[1] Kelly Chance,[2] Xiong Liu,[2,3,4] Thomas P. Kurosu,[2] and Stanley P. Sander[1]

Received 22 March 2007; revised 30 April 2007; accepted 1 June 2007; published 29 June 2007.

[1] We present retrievals of IO total columns from the Scanning Imaging Absorption Spectrometer for Atmospheric Chartography (SCIAMACHY) satellite instrument. We analyze data for October 2005 in the polar regions to demonstrate for the first time the capability to measure IO column abundances from space. During the period of analysis (*i.e.* Southern Hemisphere springtime), enhanced IO vertical columns over 3×10^{13} molecules cm^{-2} are observed around coastal Antarctica; by contrast during that time in the Artic region IO is consistently below the calculated instrumental detection limit for individual radiance spectra ($2-4 \times 10^{12}$ molecules cm^{-2} for slant columns). The levels reported here are in reasonably good agreement with previous ground-based measurements at coastal Antarctica. These results also demonstrate that IO is widespread over sea-ice covered areas in the Southern Ocean. The occurrence of elevated IO and its hitherto unrecognized spatial distribution suggest an efficient iodine activation mechanism at a synoptic scale over coastal Antarctica. **Citation:** Saiz-Lopez, A., K. Chance, X. Liu, T. P. Kurosu, and S. P. Sander (2007), First observations of iodine oxide from space, *Geophys. Res. Lett.*, *34*, L12812, doi:10.1029/2007GL030111.

1. Introduction

[2] The role of iodine in tropospheric and stratospheric chemistry has been studied intensively over the past two decades focusing on its potential to destroy O_3 in catalytic cycles [e.g., *Chameides and Davis*, 1980; *Solomon et al.*, 1994; *Vogt et al.*, 1999; *McFiggans et al.*, 2000] and its involvement in the formation of ultrafine particles in coastal marine environments [e.g., *O'Dowd et al.*, 2002; *McFiggans et al.*, 2004; *Saiz-Lopez et al.*, 2006]. IO radicals form following the photolysis of photolabile iodine species and the subsequent reaction of I atoms with atmospheric O_3. Ground-based [*Wennberg et al.*, 1997; *Alicke et al.*, 1999; *Allan et al.*, 2000; *Wittrock et al.*, 2000; *Friess et al.*, 2001; *Saiz-Lopez and Plane*, 2004; *Peters et al.*, 2005; *Zingler and Platt*, 2005; *Saiz-Lopez et al.*, 2007] and balloon-borne [*Pundt et al.*, 1998; *Bösch et al.*, 2003] instruments have measured IO in significant concentrations in the lower troposphere over a number of coastal locations although only upper limits (< 0.1 pptv) have been reported in the stratosphere. Since IO has not yet been measured by satellite-based instruments, the spatial and temporal distributions of IO on global scales are currently highly uncertain.

[3] The Scanning Imaging Absorption Spectrometer for Atmospheric Chartography (SCIAMACHY) instrument was launched on March 1, 2002 on board the European Space Agency's Envisat satellite. Envisat is in a sun synchronous polar orbit of about 800-km altitude with an equator crossing time of 10:00 a.m. in the descending node and a 100.54 minute orbital period (14.32 orbits/day). SCIAMACHY measures the continuous spectrum from 240–1700 nm at moderate spectral resolution, and has additional measurement bands in the infrared near 2 and 2.4 μm. The instrument performs a nadir and limb measurement sequence every 3.88 degrees of orbital phase so that nadir observations are made on approximately half of the daylit side of each orbit. Nadir measurements are made with a nominal spatial resolution of 30 km along-track, and with cross-track resolution varying between 30 and 120 km, depending on wavelength and latitude [*Bovensmann et al.*, 1999].

[4] This paper presents SCIAMACHY observations of IO total columns over widespread sea-ice areas around coastal Antarctica during springtime (October 2005). While SCIAMACHY was designed to provide quantitative measurements of stratospheric and tropospheric gases including O_3, NO_2 and BrO [*Chance et al.*, 1991], the IO measurements presented here demonstrate a new capability which will significantly enhance the understanding of polar tropospheric halogen chemistry.

2. Data Analysis

2.1. Spectral Fitting

[5] We determine the slant columns of IO by directly fitting SCIAMACHY radiances as described in [*Chance*, 1998], except that radiance measurements around the equator are used in lieu of solar reference measurements. This 'soft calibration' technique reduces the influence of instrument artifacts that arise from SCIAMACHY's still less-than optimum calibration [*Martin et al.*, 2002]. This approach not only removes systematic negative offset values retrieved with an irradiance reference but also improves the fitting precision by a factor of about 4. The slant column abundance that minimizes the χ^2 between measured and calculated radiance is retrieved using a non-linear least squares inversion method based on the Levenberg-Marquardt formulation [*Press et al.*, 1986]. No high-pass filtering or smoothing is implemented in the spectral analysis.

[6] Back scattered radiances are computed from the equatorial radiance reference, high resolution laboratory reference spectra for the absorbing species IO [*Spietz et*

[1]Jet Propulsion Laboratory, California Institute of Technology, Pasadena, California, USA.
[2]Atomic and Molecular Physics Division, Harvard-Smithsonian Center for Astrophysics, Cambridge, Massachusetts, USA.
[3]Now at Goddard Earth Sciences and Technology, University of Maryland Baltimore County, Baltimore, Maryland, USA.
[4]Also at NASA Goddard Space Flight Center, Greenbelt, Maryland, USA.

0094-8276/07/2007GL030111$05.00

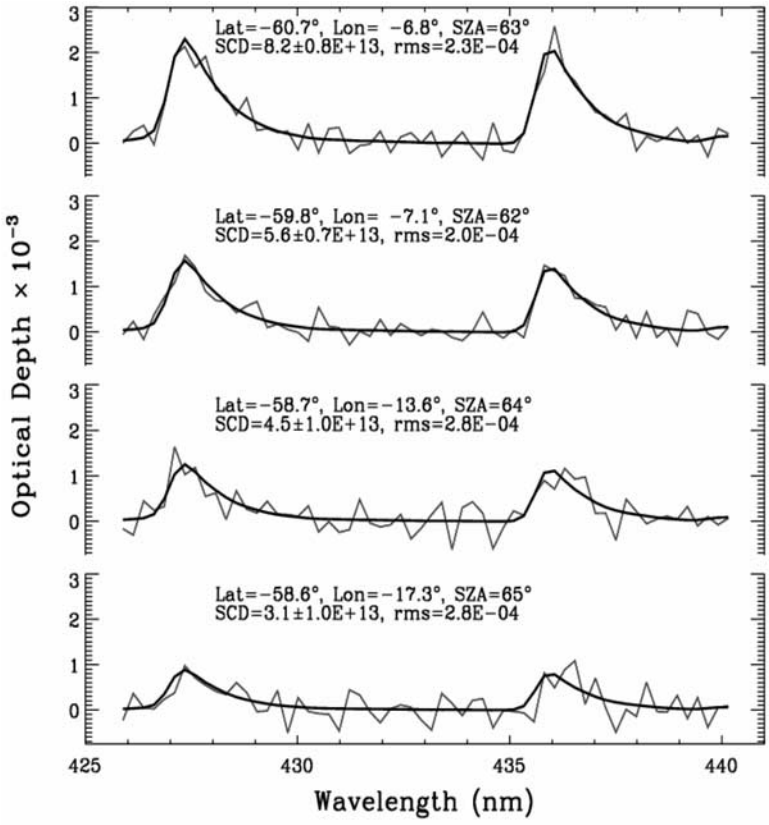

Figure 1. Examples of atmospheric spectral fits for different geographical locations and SZA along one SCIAMACHY orbit on October 5, 2005. The grey line corresponds to the fitted IO atmospheric optical density plus the final fitting residual; the black line is the fitted IO atmospheric optical density. The retrieved amounts and the 1σ fitting uncertainties are in slant column density units of molecule cm^{-2}. The fitting root mean square (rms) values are given as fractions of full-scale radiance.

al., 2005], NO_2 [*Vandaele et al.*, 2003], O_3 [*Bogumil et al.*, 2003], the O_2–O_2 collision complex [*Greenblatt et al.*, 1990], H_2O [*Rothman*, 2005], the Ring effect and the H_2O-Ring effect. The reference spectra are convolved with the SCIAMACHY instrument slit function, as determined from fits to the high-resolution solar reference spectrum for wavelength calibration [*Chance*, 1998]. The contribution of the Ring effect is calculated as the inelastic (Raman) scattering component of Rayleigh scattering of the Fraunhofer spectrum [*Chance and Spurr*, 1997]. The H_2O-Ring effect that arises from the filling-in of the solar lines by Raman scattering in the librational lines of liquid H_2O is computed as by *Martin et al.* [2002]. The detection of IO was performed using the $A^2\Pi_{3/2}$–$X^2\Pi_{3/2}$electronic transition of the radical over the wavelength window between 426 and 440 nm. The (4,0) and (3,0) bands, centered at 427 nm and 435.7 nm, respectively, were employed in the identification of IO.

[7] The SCIAMACHY solar irradiance and backscattered radiance spectra are wavelength-calibrated using the technique of cross correlation with the Fraunhofer reference spectrum [*Caspar and Chance*, 1997]. We generate two undersampling spectra, computed from the Fraunhofer reference spectrum, to account for the aliasing introduced from SCIAMACHY spectral undersampling and differences between the instrument transfer functions for solar irradiance and backscattered radiances [*Chance*, 1998; *Chance et al.*, 2005]. For each orbit we generate a common mode residual by averaging the remaining fitting residuals that contain instrumental artifacts and imperfect undersampling corrections. As with previous GOME and SCIAMACHY trace gas fitting, inclusion of the common mode residual in the spectral analysis improves the fitting precision by a factor of up to 2–3. However, the retrieved slant columns differ by less than 1 % with and without implementation of the common mode residual.

[8] Figure 1 shows examples of the fitted atmospheric IO absorption optical thickness (black line) and the sum of IO absorption thickness and radiance fitting residuals (grey line) for four different IO slant columns. Different individual radiance spectral fits for measurements in the same orbit illustrate the clear identification of IO from SCIAMACHY data. Analyses of single radiance spectra give fitting root mean square (rms) values of $2–4 \times 10^{-4}$ of the full scale radiance, corresponding to IO slant column detection limits of $2–4 \times 10^{12}$ molecules cm^{-2}. The fitting uncertainty for IO ranges from 10 to 40% depending upon IO optical thickness, surface albedo, solar zenith angle (SZA) and instrumental artifact correction.

2.2. Vertical Column Determination

[9] The light that reaches the instrument is either reflected from the Earth's surface or scattered back from the atmosphere. Hence, the retrieved slant column amounts are a function of the viewing- and SZA dependent light path

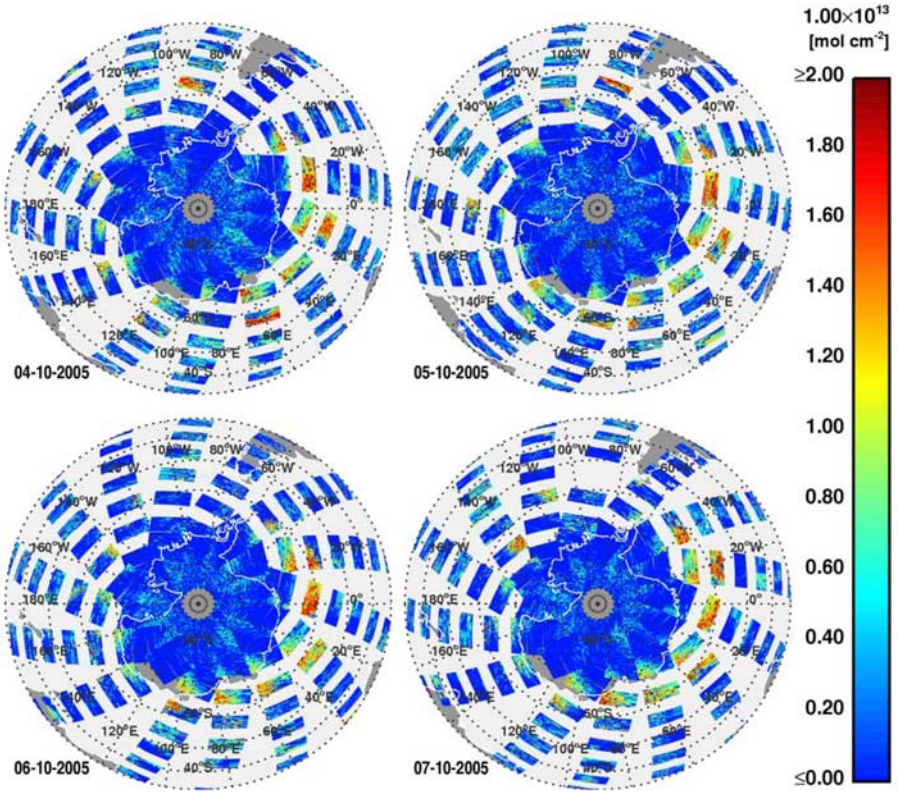

Figure 2. SCIAMACHY observations of the IO vertical column density over the Antarctic for October 4–7, 2005. The areas with enhanced IO concentrations and their temporal evolution during 4 days are clearly visible around the Antarctic continent. Note that the white areas on the map correspond to times in which no satellite nadir data is available either due to the non-global coverage or because the instrument is observing in limb mode.

through the atmosphere. The IO vertical columns are obtained by inverting the line-of-sight slant column observations using a geometric air mass factor (AMF = 1/cos (SZA) + 1/cos (VZA), where VZA is viewing zenith angle; AMF = slant column/vertical column). The AMF represents a potential source of systematic error in the retrieval because it depends on uncertain parameters such as the IO vertical profile, surface albedo, and cloud properties. Using a radiative transfer model (LIDORT) [*Spurr et al.*, 2001] we find that if IO is well mixed in the 1-km layer, at 60° SZA and albedo of 0.6 – 0.9, the AMF varies by less than 20 %. Most of this information can be determined directly from the SCIAMACHY data. For example, the SZA dependence of the observed IO optical depth places constraints on the vertical concentration profile. For a stratospheric absorber there would be a strong increase in the slant column with increasing SZA, while for a lower tropospheric constituent the geometric dependence with SZA is considerably weaker. Our observations show that the retrieved slant columns rapidly decrease with increasing SZA (> 80°) as the satellite moves poleward. Sensitivity in lower troposphere decreases with increasing SZA due to Rayleigh scattering impact on the seeing which, unlike in the stratosphere, more than offsets the geometric advantage.

3. Results and Discussion

[10] Figure 2 shows the distribution of IO in the Southern Hemisphere for 4–7 October 2005 as retrieved from SCIAMACHY nadir observations. Gaps between subsequent nadir observations (North-to-South direction) correspond to periods of limb measurements. Large enhancements are observed over sea-ice areas of the Southern Ocean and around the edge of the Antarctic ice shelf. IO vertical columns of more than 3×10^{13} molecules cm^{-2} were measured by SCIAMACHY in October. Assuming that the bulk of IO is only contained, and well mixed, within the first kilometer of the atmosphere we estimate IO concentrations over 3×10^{8} molecules cm^{-3}. These values correspond to IO mixing ratios in excess of 12 ppt in agreement with ground-based measurements during the Antarctic springtime [*Friess et al.*, 2001; *Saiz-Lopez et al.*, 2007]. Note however that the variability in the boundary layer thickness is considerable over coastal Antarctica, ranging from hundreds of meters to $\sim$ 2 km [*Anderson*, 2003] implying even higher or lower IO concentrations corresponding to the observed vertical columns. Hence, combined knowledge of the vertical distribution of the molecule in the atmosphere and information on boundary layer meteorology are needed to validate the satellite observations with correlative measurements from the ground.

[11] In the Southern Hemisphere, during the entire month of October 2005, enhanced IO columns are observed in the same latitude range (from about 55°S to 78°S) as the sea-ice covered area surrounding the Antarctic continent. The measurements show that the total area of elevated IO

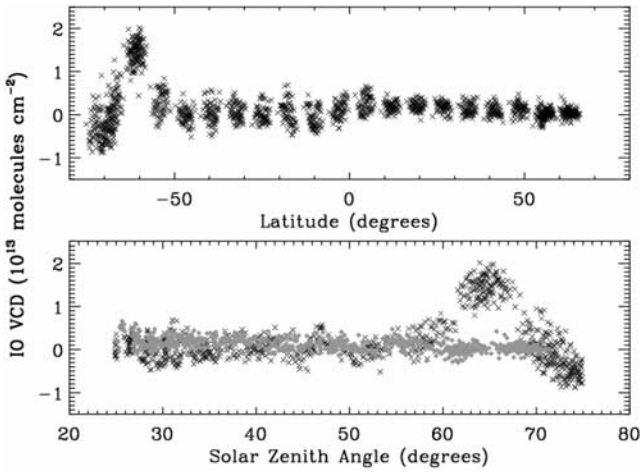

Figure 3. A cross-section through the global IO vertical columns along one SCIAMACHY orbit. (top) IO is plotted as a function of latitude to show the comparatively large enhancement of IO concentrations between 60° and 70° south; by contrast in the Arctic, IO is not observed at significant levels during this time of year. (bottom) The dependence of the IO column with SZA (cross symbol: Southern Hemisphere; solid diamond: Northern Hemisphere). The apparent negative values at highest SZA are right at the extreme of our sensitivity: instrumental factors will become more prominent with decreasing signal-to-noise ratios at large SZA.

concentrations around the Antarctic extends up to about 1×10^7 km^2 during springtime. By contrast, in the Northern Hemisphere high IO columns are not apparent during this time of year.

[12] These results demonstrate that IO is as widespread around coastal Antarctica as previous satellite observations have shown to be the case for BrO [e.g., *Hollwedel et al.*, 2004]. Our measurements also largely support speculations, based on recent findings [*Saiz-Lopez et al.*, 2007], that suggest the occurrence of an iodine activation mechanism efficient at a regional scale over coastal Antarctica.

[13] An illustration of a cross-section through the latitudinal distribution of IO for one individual orbit (October 5th) is given in Figure 3. In Figure 3 (top), it can be seen that at this time of year IO is not detectable in the Arctic; by contrast in the Southern Hemisphere the retrieved amount shows an obvious increase between 60°S and 70°S. The Antarctic/Arctic seasonality is consistent with what is seen for BrO [*Hollwedel et al.*, 2004]. The bottom panel shows the dependence of IO vertical columns on SZA for both hemispheres. Note that while in the north there is not retrievable IO, in the Antarctic the peak value occurs at SZA 65° and it subsequently decays with larger SZA. We thus suggest that this dependence with SZA in early October may be due to two factors: i) the possibility that the tropospheric IO enhancements are geographically localized, ii) the decreasing sensitivity of the nadir viewing geometry with increasing SZA for an absorber located in the lower troposphere. Nevertheless, the SZA dependence can only be taken into account to the extent that we know the IO profile. Lack of that knowledge causes uncertainty that grows with SZA.

[14] The sources and mechanisms of such a large burden of IO over the Southern Ocean areas are not yet understood. However, in contrast to ground-based measurements, the satellite observations reported here provide valuable information on the spatial and temporal distribution of the episodes of IO enhancements in the troposphere. This will therefore further our understanding of the geographical locations and the environmental conditions under which reactive iodine chemistry leads to the observed enhanced abundance of IO. The measurement of the global distributions of IO will also contribute to a more comprehensive evaluation of the potential role of iodine in global tropospheric chemistry.

4. Conclusions

[15] The results reported here demonstrate that IO columns can be measured globally from SCIAMACHY data, with a detection limit for slant columns of $2-4 \times 10^{12}$ molecules cm^{-2}. It is thus possible to monitor the spatial and temporal evolution of enhanced IO concentrations on a global scale with sufficient accuracy to improve our understanding of iodine chemistry in polar atmospheres. Elevated columns of IO, most likely located in the lower troposphere, are observed in the springtime over large areas of sea ice around the Antarctic continent. The widespread distribution of IO indicates an efficient iodine activation mechanism that is not yet understood. Our ongoing and future work with SCIAMACHY IO data includes: i) Development of the global climatology of IO including seasonal and northern-southern hemisphere differences; ii) Radiative transfer calculations to improve the determination of vertical columns from line-of-sight observations; iii) Comparison and validation of IO vertical columns with ground-based instrumentation.

[16] **Acknowledgments.** A. Saiz-Lopez was supported by an appointment to the NASA Postdoctoral Program at the Jet Propulsion Laboratory, administered by Oak Ridge Associated Universities through a contract with the National Aeronautics and Space Administration (NASA). Research at the Jet Propulsion Laboratory, California Institute of Technology, under a contract with NASA, was supported by the NASA Upper Atmosphere Research and Tropospheric Chemistry Programs. Research at the Smithsonian Astrophysical Observatory was supported by NASA and the Smithsonian Institution. We thank Chris Sioris for providing help with SCIAMACHY data. We are also grateful for the ongoing cooperation of the European Space Agency and the German Aerospace Center in the SCIAMACHY program.

References

Alicke, B., K. Hebestreit, J. Stutz, and U. Platt (1999), Iodine oxide in the marine boundary layer, *Nature*, *397*, 572–573.

Allan, B. J., G. McFiggans, J. M. C. Plane, and H. Coe (2000), Observations of iodine monoxide in the remote marine boundary layer, *J. Geophys. Res.*, *105*, 14,363–14,369.

Anderson, P. S. (2003), Fine-scale structure observed in a stable atmospheric boundary layer by Sodar and kite-borne tethersonde, *Boundary Layer Meteorol.*, *107*, 323–351.

Bogumil, K., et al. (2003), Measurements of molecular absorption spectra with the SCIAMACHY pre-flight model: Instrument characterization and reference data for atmospheric remote-sensing in the 230–2380 nm region, *J. Photochem. Photobiol. A Chem.*, *157*(2–3), 167–184.

Bösch, H., C. Camy-Peyret, M. P. Chipperfield, R. Fitzenberger, H. Harder, U. Platt, and K. Pfeilsticker (2003), Upper limits of stratospheric IO and OIO inferred from center- to-limb-darkening-corrected balloon-borne solar occultation visible spectra: Implications for total gaseous iodine and stratospheric ozone, *J. Geophys. Res.*, *108*(D15), 4455, doi:10.1029/2002JD003078.

Bovensmann, H., J. P. Burrows, M. Buchwitz, J. Frerick, S. Noël, V. V. Rozanov, K. V. Chance, and A. P. H. Goede (1999), SCIAMACHY: Mission objectives and measurement modes, *J. Atmos. Sci.*, *56*, 127–150.

Caspar, C., and K. Chance (1997), GOME wavelength calibration using solar and atmospheric spectra, in *Proceedings of the Third ERS Symposium on Space at the Service of our Environment*, edited by T.-D. Guyenne and D. Danesy, *Publ. SP-414*, Eur. Space Agency, Paris.

Chameides, W. L., and D. D. Davis (1980), Iodine: Its possible role in tropospheric photochemistry, *J. Geophys. Res.*, *85*, 7383–7393.

Chance, K. (1998), Analysis of BrO measurements from the Global Ozone Monitoring Experiment, *Geophys. Res. Lett.*, *25*, 3335–3338.

Chance, K. V., and R. J. D. Spurr (1997), Ring effect studies: Rayleigh scattering, including molecular parameters for rotational Raman scattering, and the Fraunhofer spectrum, *Appl. Opt.*, *36*, 5224–5230.

Chance, K. V., J. P. Burrows, and W. Schneider (1991), Retrieval and molecule sensitivity studies for the Global Ozone Monitoring Experiment and the Scanning Imaging Absorption spectroMeter for Atmospheric CHartographY, *Proc. SPIE Remote Sens. Atmos. Chem.*, *1491*, 151–165.

Chance, K., T. P. Kurosu, and C. E. Sioris (2005), Undersampling correction for array-detector based satellite spectrometers, *Appl. Opt.*, *44*, 1296–1304.

Friess, U., T. Wagner, I. Pundt, K. Pfeilsticker, and U. Platt (2001), Spectroscopic measurements of tropospheric iodine oxide at Neumayer Station, Antarctica, *Geophys. Res. Lett.*, *28*, 1941–1944.

Greenblatt, G. D., J. J. Orlando, J. B. Burkholder, and A. R. Ravishankara (1990), Absorption measurements of oxygen between 330 and 1140 nm, *J. Geophys. Res.*, *95*, 18,577–18,582.

Hollwedel, J., M. Wenig, S. Beirle, S. Kraus, S. Kuhl, W. Wilms-Grabe, U. Platt, and T. Wagner (2004), Year-to-year variations of spring time polar tropospheric BrO as seen by GOME, *Adv. Space Res.*, *34*, 804–808.

Martin, R. V., et al. (2002), An improved retrieval of tropospheric nitrogen dioxide from GOME, *J. Geophys. Res.*, *107*(D20), 4437, doi:10.1029/2001JD001027.

McFiggans, G., J. M. C. Plane, B. J. Allan, L. J. Carpenter, H. Coe, and C. D. O'Dowd (2000), A modeling study of iodine chemistry in the marine boundary layer, *J. Geophys. Res.*, *105*, 14,371–14,385.

McFiggans, G., et al. (2004), Direct evidence for coastal iodine particles from Laminaria macroalgae—Linkage to emissions of molecular iodine, *Atmos. Chem. Phys.*, *4*, 701–713.

O'Dowd, C. D., et al. (2002), Marine aerosol formation from biogenic iodine emissions, *Nature*, *417*, 632–636.

Peters, C., S. Pechtl, J. Stutz, K. Hebestreit, G. Honninger, K. G. Heumann, A. Schwarz, J. Winterlik, and U. Platt (2005), Reactive and organic halogen species in three different European coastal environments, *Atmos. Chem. Phys.*, *5*, 3357–3375.

Press, W. H., T. S. Flannery, and W. T. Vetterling (1986), *Numerical Recipes: The Art of Scientific Computing*, Cambridge Univ. Press, New York.

Pundt, I., J. P. Pommereau, C. Phillips, and E. Lateltin (1998), Upper limit of iodine oxide in the lower stratosphere, *J. Atmos. Chem.*, *30*, 173–185.

Rothman, L. S. (2005), HITRAN 2004 molecular spectroscopic database, *J. Quant. Spectrosc. Radiat. Transfer*, *96*, 139–204.

Saiz-Lopez, A., and J. M. C. Plane (2004), Novel iodine chemistry in the marine boundary layer, *Geophys. Res. Lett.*, *31*, L04112, doi:10.1029/2003GL019215.

Saiz-Lopez, A., J. M. C. Plane, G. McFiggans, P. I. Williams, S. M. Ball, M. Bitter, R. L. Jones, C. Hongwei, and T. Hoffmann (2006), Modelling molecular iodine emissions in a coastal marine environment: The link to new particle formation, *Atmos. Chem. Phys.*, *6*, 883–895.

Saiz-Lopez, A., A. S. Mahajan, R. A. Salmon, S. J.-B. Bauguitte, A. E. Jones, H. K. Roscoe, and J. M. C. Plane (2007), Boundary layer halogens in coastal Antarctica, *Science*, in press.

Solomon, S., R. R. Garcia, and A. R. Ravishankara (1994), On the role of iodine in ozone depletion, *J. Geophys. Res.*, *99*, 20,491–20,500.

Spietz, P., J. C. Gomez-Martin, and J. P. Burrows (2005), Spectroscopic studies of the I_2/O_3 photochemistry: Part 2. Improved spectra of iodine oxides and analysis of the IO absorption, *J. Photochem. Photobiol. A Chem.*, *176*, 50–67.

Spurr, R. J. D., T. P. Kurosu, and K. Chance (2001), A linearized discrete ordinate radiative transfer model for atmospheric remote sensing retrieval, *J. Quant. Spectrosc. Radiat. Transfer*, *68*, 689–735.

Vandaele, A. C., C. Hermans, S. Fally, M. Carleer, M.-F. Merienne, A. Jenouvrier, B. Coquart, and R. Colin (2003), Absorption cross-sections of NO_2: Simulation of temperature and pressure effects, *J. Quant. Spectrosc. Radiat. Transfer*, *76*, 373–391.

Vogt, R., R. Sander, R. von Glasow, and P. J. Crutzen (1999), Iodine chemistry and its role in halogen activation and ozone loss in the marine boundary layer: A model study, *J. Atmos. Chem.*, *32*, 375–395.

Wennberg, P. O., J. W. Brault, T. F. Hanisco, R. J. Salawitch, and G. H. Mount (1997), The atmospheric column abundance of IO: implications for stratospheric ozone, *J. Geophys. Res.*, *102*, 8887–8898.

Wittrock, F., R. Muller, A. Richter, H. Bovensmann, and J. P. Burrows (2000), Measurements of iodine monoxide (IO) above Spitsbergen, *Geophys. Res. Lett.*, *27*, 1471–1474.

Zingler, J., and U. Platt (2005), Iodine oxide in the Dead Sea Valley: Evidence for inorganic source of boundary layer IO, *J. Geophys. Res.*, *110*, D07307, doi:10.1029/2004JD004993.

K. Chance and T. P. Kurosu, Atomic and Molecular Physics Division, Harvard-Smithsonian Center for Astrophysics, Cambridge, MA 02138, USA.

X. Liu, Goddard Earth Sciences and Technology, University of Maryland Baltimore County, Baltimore, MD 21250, USA.

A. Saiz-Lopez and S. P. Sander, Earth and Space Science Division, Jet Propulsion Laboratory, California Institute of Technology, Pasadena, CA 91109, USA. (alfonso.saiz-lopez@jpl.nasa.gov)